J Nanostruct 16(2): 2357-2369, Spring 2026

RESEARCH PAPER

# $Fe_3O_4$@Nano-Coconout Shell/Cu(II) as a Unique, High Efficient and Reusable Natural Based Nano-Catalyst for Synthesis of Polyhydroquinolines

*Farhad Hajati [1], Bi Bi Fatemeh Mirjalili [1] *, Abdolhamid Bamoniri [2]*

[1] *Department of Organic Chemistry, Faculty of Chemistry, College of Science, Yazd University, P. O. Box 89195-741, Postal code 8915813149, Yazd, Iran*

[2] *Department of Organic Chemistry, Faculty of Chemistry, University of Kashan, Kashan, Iran*

## ARTICLE INFO

***Article History:***
*Received 25 November 2025*
*Accepted 27 March 2025*
*Published 01 April 2026*

***Keywords:***
*Green Chemistry*
*$Fe_3O_4$@nano-coconout shell / Cu(II)*
*Multi-component reactions*
*Nano-coconout shell*
*Polyhydroquinolines*

## ABSTRACT

Polysaccharides are the most plentiful biopolymers in nature, which are abundantly in nature. Biopolymers such as coconut shell's cellulose is a biocompatible, renewable and biodegradable material. The OH groups in cellulose section of coconot shell act as nucleophile for binding to metal ions. $Fe_3O_4$@nano-coconout shell /Cu(II) catalyst was synthesized and characterized by different techniques such as FTIR, FESEM, TEM, EDX, MAPPING, BET and TGA. According to different analysis, $Fe_3O_4$@nano-coconout shell /Cu(II) has good stability under heating with particle size under 50 nm. Polyhydroquinolines as significant nitrogen-containing compounds have excellent pharmaceutical applications. In this research work, $Fe_3O_4$@nano-coconout shell /Cu(II) was applied for the synthesis of Polyhydroquinoline derivatives. Polyhydroquinoline were synthesized *via* reaction of aldehyde, dimedone, ethyl acetoacetate and ammonium acetate under solvent-free condition using an electrical mortar-heater. This protocol has some advantages such as simple operation and work up, high yields of products, reusability of catalyst with no any leaching in reaction mixture.

**How to cite this article**
*Hajati F., Mirjalili B.., Bamoniri A. $Fe_3O_4$@Nano-Coconout Shell/Cu(II) as a Unique, High Efficient and Reusable Natural Based Nano-Catalyst for Synthesis of Polyhydroquinolines J Nanostruct, 2026; 16(2):2357-2369. DOI: 10.22052/JNS.2026.02.079*

## INTRODUCTION

In recent decades, the synthesis and utilization of naturally occurring catalysts have become a serious study subject in following of green chemistry principles.

Polysaccharides are the most plentiful biopolymers in nature, which are abundantly found in plants and animals, microorganisms, microalgae, bacteria and fungi [1].

Biopolymers such as coconut shell's cellulose is a biocompatible, renewable and biodegradable material containing OH groups [2-7]. $Fe_3O_4$ nanoparticles are coated with various materials such as surfactants [8], polymers [9,10], silica [11], cellulose [12] and carbon [13] to form core–shell structures. Magnetic nanoparticles as heterogeneous catalyst have many advantages such as high dispersion in reaction media and easy recovery by an external magnet [14]. Cu(II) as a safe and ecofriendly cation is a good Lewis acid and can activate the carbonyl group for nucleophilic addition reactions [15]. The presence of large

* *Corresponding Author Email: fmirjalili@yazd.ac.ir*

numbers of polar hydroxyl groups, cellulose can be coordinated to many metal ions ($Mg^{2+}$, $Ca^{2+}$, $Pb^{2+}$, $Cu^{2+}$, and $Co^{3+}$) [16–19].

Polyhydroquinoline (PHQ) derivatives are significant nitrogen-containing compounds. Some of them possess antitumor, anticancer, neurotropic, neuropeptide, hepatoprotective, neuroprotective, vasodilator, platelet anti-aggregation, antidiabetic activity and bronchodilator [20-21]. Various catalysts such as [Msim]Cl [22], nano-$Fe_3O_4$@dextrin/$BF_3$ [23], $CeO_2$-$ZrO_2$ [24], V–$TiO_2$ [25], IRMOF-3 [26], $Yb(OTF)_3$ [27], $Cs_{2.5}H_{0.5}PW_{12}O_{40}$ [28], $LaCl_3.7H_20$ [29]and NiO-$ZrO_2$ [30] have been applied for synthesis of polyhydroquinoline derivatives.

In this study, $Fe_3O_4$@nano-coconut shell/Cu(II) was prepared as a natural based, biocompatible and green magnetic nano-catalyst. And its effects considered in the reaction of aldehyde, dimedone, ethyl acetoacetate and ammonium acetate for the synthesis of polyhydroquinoline derivatives (PHQs) (Fig. 1 (a, b)).

## MATERIALS AND METHODS

### *General*

All chemical materials were purchased from Aldrich, Merck and Fluka chemical companies. The synthesized magnetic nanocatalyst were

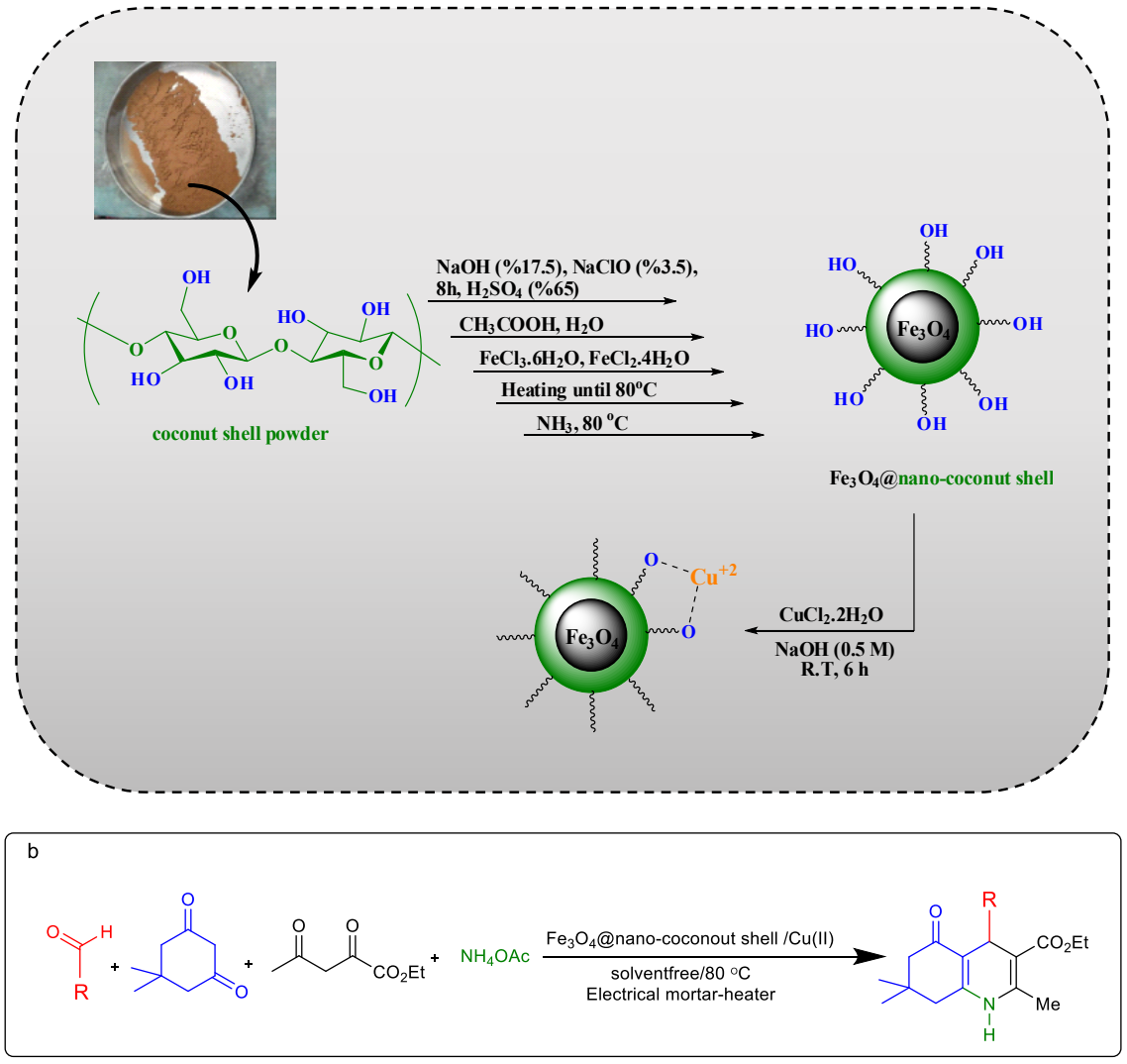


Fig. 1. Preparation of (a) $Fe_3O_4$@nano-coconout shell/Cu(II) and (b) Synthesis of polyhydroquinoline derivatives catalyzed by $Fe_3O_4$@nano-Coconout shell /Cu(II)

characterized by FT-IR spectra (Bruker, Equinox 55 spectrometer). The $^1$H-NMR spectrum was measured on a Bruker (DRX-400 Avance) NMR. Melting points were measured on a Buchi melting point B-540 B.V.CHI instrument and uncorrected. X-ray diffraction (XRD) pattern was obtained by a Philips Xpert MPD diffract meter equipped with a Cu Kα anode (k = 1.54 Å) in the 2θ range from 10 to 80 °. Field Emission Scanning Electron Microscopy (FESEM) was obtained on a Mira 3-XMU. XRF analysis was done with Bruker, S4 Explorer instrument. The magnetization of the prepared catalyst was characterized by using a Vibrating Sample Magnetometer (Meghnatis Daghigh Kavir Co. Kashan, I.R.IRAN). Quantitative elemental information and maps of catalyst was studied *via* energy-dispersive X-Ray spectroscopy (EDX) by a Phenom pro X instrument. BELSORP MINI II nitrogen adsorption apparatus (Japan) was used for recording of Brunauer–Emmett–Teller (BET) specific surface area of catalyst at 77 K.

*Preparation of nano-coconut shell*

To prepare the nano-coconut shell, the Coconut shell was heated in boiling water for 30 minutes, dried, and powdered. The next, treated with a 17.5 w/v NaOH solution at 90°C for 24 h under reflux condition. Subsequently, the Coconut shell was filtered and washed with distilled water. Then, bleached with 100 mL of 1:1 aqueous dilution of 3.5% w/v sodium hypochlorite (NaOCl) at 80 °C for 3 h under reflux condition. The resulting powder was hydrolyzed partially using 35% sulfuric acid ($H_2SO_4$) aqueous solution with a Coconut shell-to-acid weight ratio of 1–10 at 45 °C. After 3 h, the obtained suspension was diluted with water five-fold to stop the hydrolysis reaction. The suspension was centrifuged at 4000 rpm to separate the nano-coconut shell from the acid solution (yield 65%).

*Preparation of $Fe_3O_4$@nano-coconut shell*

1.5 g of nano-coconut shell powder was poured in 100 mL of 0.05 M acetic acid solution; Then, $FeCl_3.6H_2O$ (3.51 g, 0.013 mol) and $FeCl_2.4H_2O$ (1.29 g, 0.0065 mol) were added to it. The mixture was stirred for 6 h at 80 °C. As a result, 6 mL of 25% $NH_4OH$ was added dropwise into the reaction mixture with constant stirring. After 30 min, the mixture was cooled to room temperature. Then $Fe_3O_4$@nano-coconut shell was separated by using an external magnet, washed with distilled water and dried at 80 °C for 4 h. The weight of the nano-$Fe_3O_4$@almond shell obtained is 2.073 g.

*Preparation of $Fe_3O_4$@nano-coconut shell/Cu(II)*

$CuCl_2$ (75 mL, 0.04 M) was added to the mixture

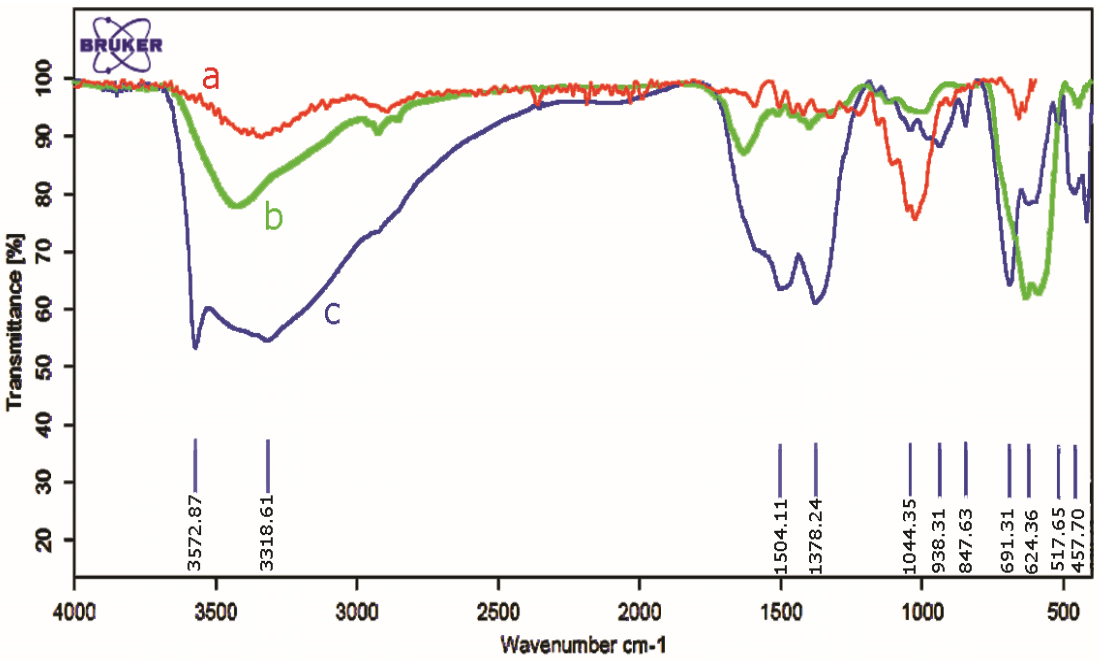


Fig. 2. FT-IR (ATR) spectra of (a) nano-coconut shell (b $Fe_3O_4$@nano-coconut shell, (c) $Fe_3O_4$@nano-coconut shell/Cu(II)

of $Fe_3O_4$@nano-coconut (1 g) in ethanol (20 mL). The reaction mixture was stirred for six hours at room temperature. The resulted magnetic nanocatalyst was washed with ethanol and water, filtered and then dried in an oven at 80 °C.

*Synthesis of polyhydroquinolines in the presence of $Fe_3O_4$@nano-coconut shell/Cu(II)*

To the mixture of ethyl acetoacetate (1mmol), aldehyde (1mmol), dimedon (1mmol) and $NH_4OAc$ (1.3mmol), $Fe_3O_4$@nano- coconut shell/Cu(II) (0.03 g) was added. The reaction mixture was stirred under the solvent-free condition at 80 °C with an electrical mortar-heater. After completion of the reaction (as monitored by TLC (hexane/ethyl acetate 4:1)), the reaction mixture was colden to room temperature and dissolved in ethanol. The $Fe_3O_4$@nano-coconut shell/Cu(II) catalyst was separated by using an external magnet. Thereafter, by pouring crushed ice on to the obtained mixture, the product was precipitated. For further purification, the solid product was recrystallized from methanol. The recovered catalyst was washed with water and ethanol, dried in an oven at 60°C and reused for subsequent runs.

*Hot filtration test*

The leaching of $Fe_3O_4$@nano-coconut shell/Cu(II) in the reaction mixture was studied using the hot filtration test. The hot filtration test was performed for the synthesis of PHQs using benzaldehyde, ethyl acetoacetate, dimedon and $NH_4OAc$ as a model reaction under the optimal reaction conditions. After the half-reaction time (7.5 min), the progress of reaction was obtained 78% by TLC . Then, the catalyst was separated from the mixture, and the reaction was continued for 7.5 minutes. We have found that the progress of reaction was terminated. These evidences show that the catalyst is stable under reaction condition with no any leaching.

*Spectral data for selected compounds*

*Ethyl 2,7,7-trimethyl-4–(4-nitrophenyl)–5-oxo-1,4,5,6,7,8-hexahydroquinoline-3-carboxylate(4n)*

Yellow solid, Mp: 234-236°C (lit. 234-236°C [31]).

IR (ATR) ῡ($cm^{-1}$):3277 (NH), 1702 (C=O, ester), 1607 (C=O, dimedone), 1518 ($NO_2$), 1492 (C=C, aromatic), 1345 ($NO_2$), 1216(C-O). $^1$H NMR (400 MHz, $CDCl_3$): δ =8.08 (d, *J* =7.9 Hz, 2H, Ar-H), 7.48 (d, *J*= 7.9 Hz, 2H, Ar-H), 5.91 (s, 1H, NH), 5.15 (s, 1H, CH), 4.05 (q, *J*= 7.1 Hz, 2H, $OCH_2$), 2.42 (s, 3H, $CH_3$), 2.10–2.36 (m, 4H, 2 $CH_2$), 1.17 (t, *J*= 7.1 Hz, 3H, $CH_3CH_2$), 1.09 (s, 3H, $CH_3$), 0.91 (s, 3H, $CH_3$). $^{13}$C NMR (100 MHz, $CDCl_3$): δ(ppm)= 195.84, 167.03,

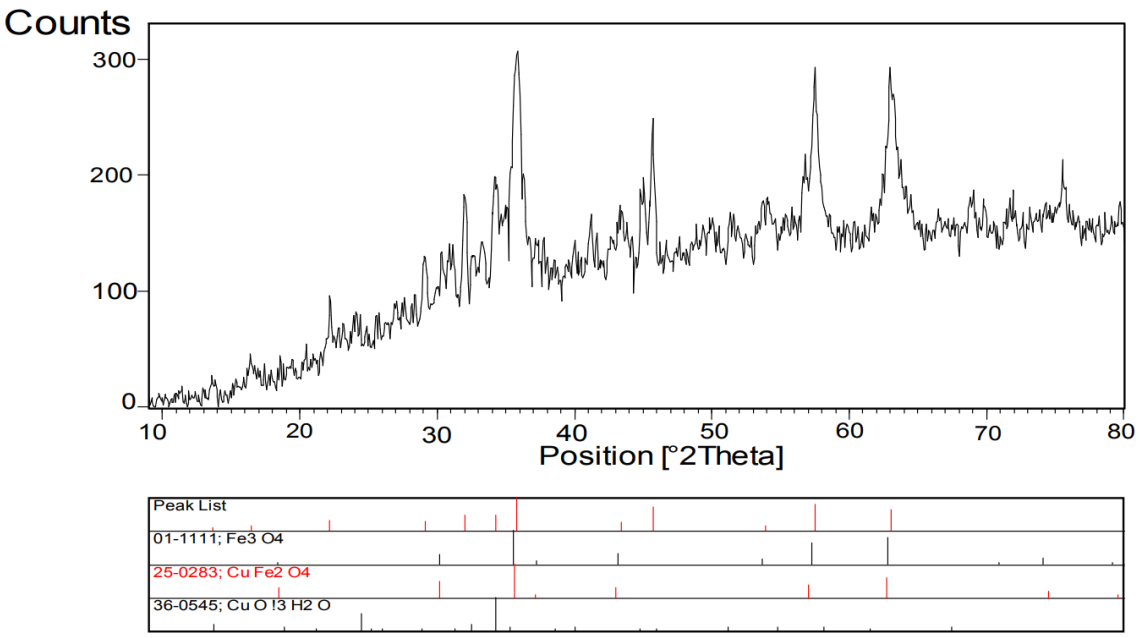


Fig. 3. XRD patterns of the $Fe_3O_4$@nano-coconut shell/Cu(II).

154.72, 150.16, 146.11,145.10, 128.97, 123.28, 110.55, 104.59, 58.22, 50.64, 40.60, 37.30, 32.62, 29.37, 26.98, 19.16, 14.21.

*Ethyl 2,7,7-Trimethyl-5-oxo-4-phenyl-1,4,5,6,7,8-hexahydroquinoline-3-carboxylate(4a)*

Yellowish solid, Mp: 223-224°C (lit. 223-225°C [31]).

IR (ATR) ῡ($cm^{-1}$): 3187 (NH), 1701 (C=O, ester), 1605 (C=O, dimedone), 1489 (C=C, aromatic), 1213 (C-O). $^1$H NMR (400 MHz, $CDCl_3$): δ =7.29 (m, *J* = 7.5 Hz, 2H, Ar-H), 7.19 (t, *J* = 7.5 Hz, 2H, Ar-H), 7.09 (t, *J* = 7.2 Hz, 1H, Ar-H), 6.44 (s, 1H, NH), 5.05 (s, 1H, CH), 4.06 (q, *J*=7.2 Hz, 2H, $OCH_2$), 2.35 (s,

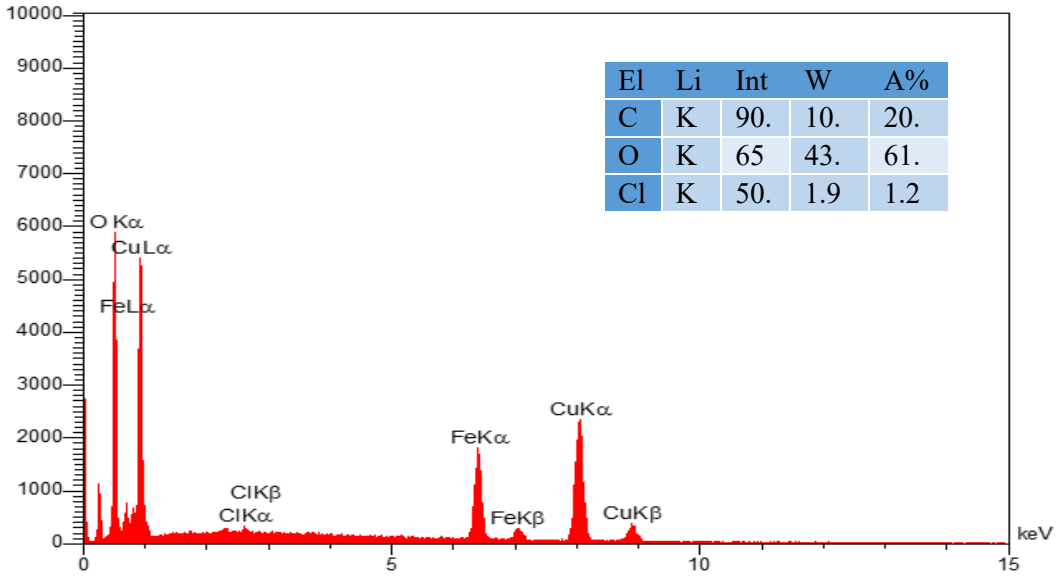


Fig. 4. EDX analysis spectra of $Fe_3O_4$@nano-coconut shell/Cu(II)

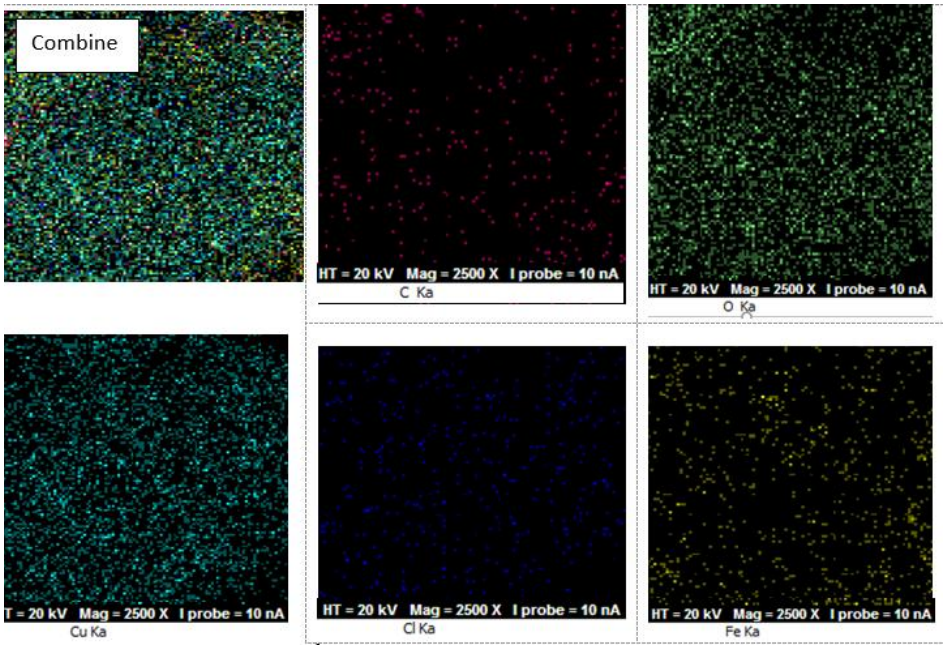


Fig. 5. Elements mapping images of $Fe_3O_4$@nano-coconut shell/Cu(II(

3H, $CH_3$), 2.13–2.30 (m, 4H, 2 $CH_2$), 1.18 (t, *J*=7.2 Hz, 3H, $CH_3CH_2$), 1.07 (s, 3H,$CH_3$), 0.93 (s, 3H, $CH_3$).

## RESULTS AND DISCUSSION

Firstly, chemical co-precipitation of $Fe^{+3}$ and $Fe^{+2}$ ions in presence of nano-coconut shell as natural source of cellulose, $Fe_3O_4$@nano-coconut shell was prepared. In the next step, $Fe_3O_4$@nano-coconut shell was used as a support for binding of Cu(II) to form $Fe_3O_4$@nano- coconut shell/Cu(II). The structure of $Fe_3O_4$@nano- coconut shell/Cu(II) as a novel natural-based magnetic nano-catalyst was investigated by TEM, SEM, FT-IR, XRD, VSM, BET, MAP and EDS techniques.

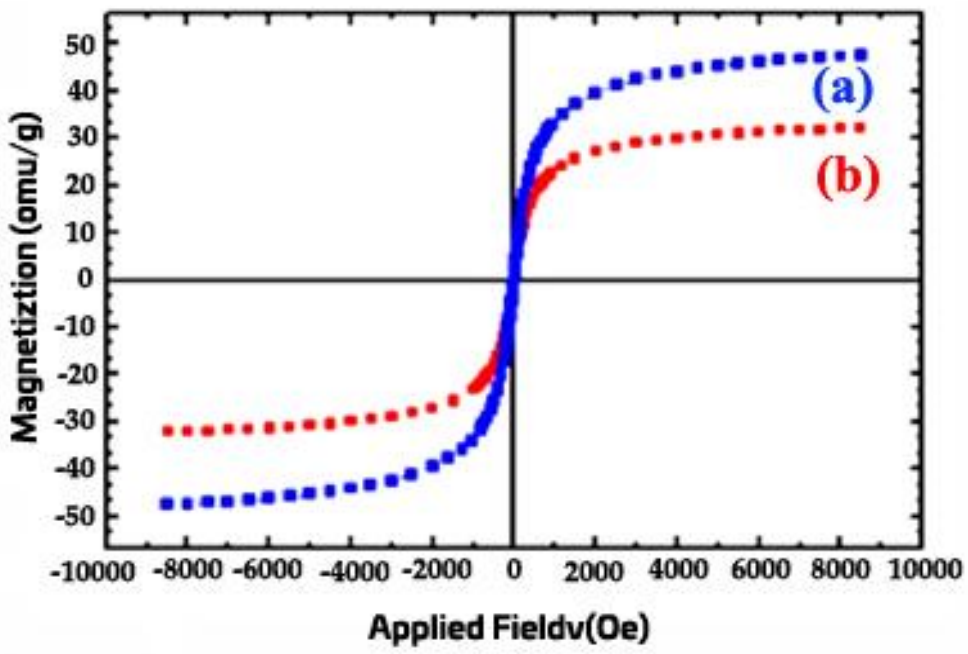


Fig. 6. Magnetization loops of (a) $Fe_3O_4$ and (b) $Fe_3O_4$@nano-coconut shell/Cu(II)

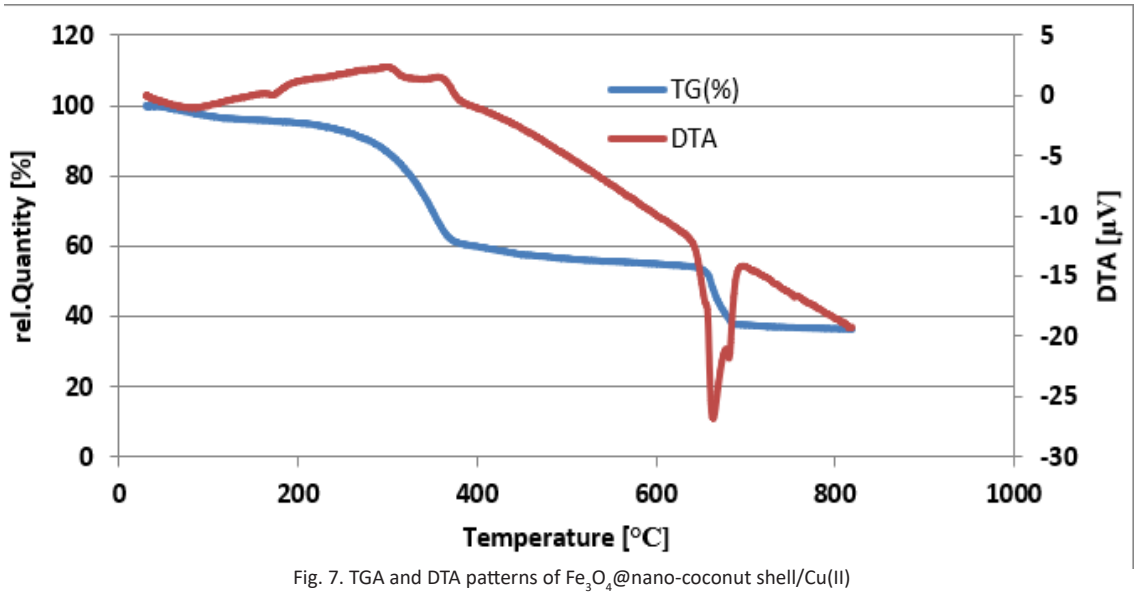


Fig. 7. TGA and DTA patterns of $Fe_3O_4$@nano-coconut shell/Cu(II)

*Characterization of the prepared catalyst*

*FT-IR Analysis*

For identification of the structure of $Fe_3O_4$@nano-coconut shell/Cu(II), FT-IR (ATR) spectra of (a) coconut shell (b) $Fe_3O_4$@nano-coconut shell, (c) $Fe_3O_4$@nano-coconut shell/Cu(II) were recorded (Fig. 2). The FT-IR spectrum of nano-coconut shell shows a broad band at 3250-3450 $cm^{-1}$ which related to the stretching vibrations of OH groups. The absorption band at 2950 $cm^{-1}$ is attributed to C-H aliphatic bonds. The absorption band around 1044 $cm^{-1}$ is due to the C–O bonds` stretching vibrations. For $Fe_3O_4$@nano-coconut shell, the absorption at 624 $cm^{-1}$ indicates the Fe/O groups` stretching vibrations that shows the magnetic $Fe_3O_4$ is coated by nano-coconut shell. The peak at 1504 $cm^{-1}$ is associated with the bending vibration of H–O–H that catalyst adsorbed water. The absorption bands at 691 $cm^{-1}$ that may be attributed to Cu-O band.

*XRD analysis*

The $Fe_3O_4$@nano-coconut shell/Cu(II) XRD pattern in a range of 10–80 ° was shown in Fig. 3.

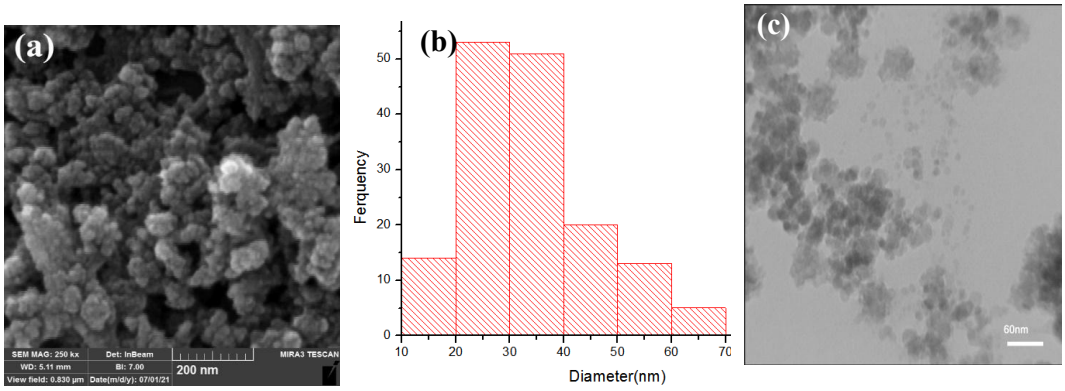


Fig. 8. (a) FESEM (b) histogram and (c)TEM images of $Fe_3O_4$@nano-coconut shell/Cu(II).

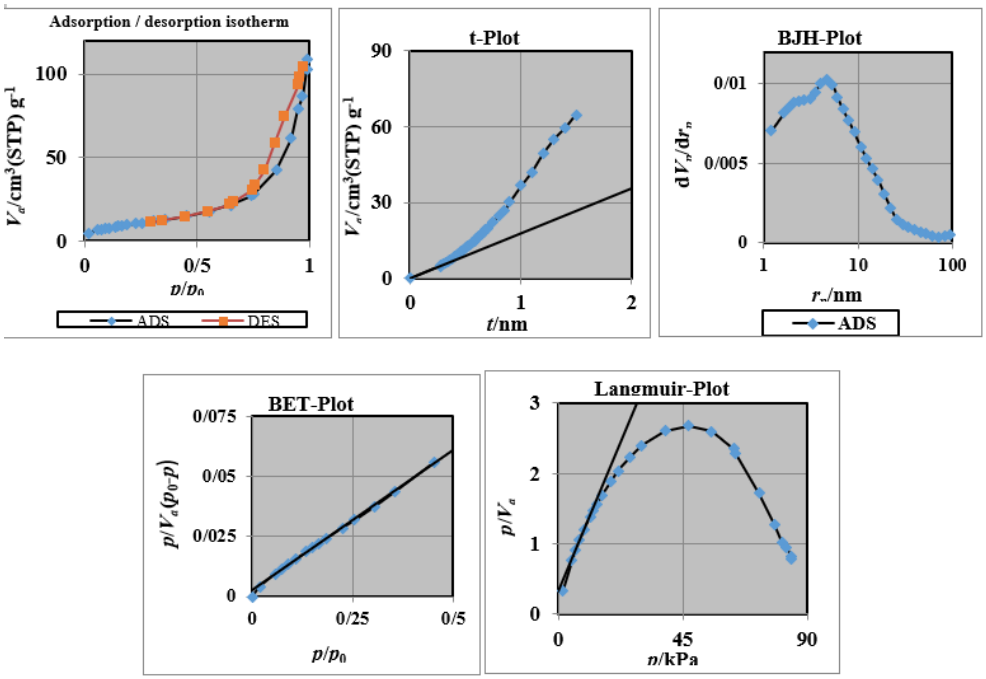


Fig. 9. $N_2$ adsorption (black line) - desorption (orang line) isotherm and corresponding diagrams

In this pattern, in addition to all peaks of naked $Fe_3O_4$ ($2\vartheta = 30^\circ, 37^\circ, 43^\circ, 53^\circ, 57^\circ, 63^\circ, 71^\circ$ and $73^\circ$), the additional diffraction peaks at $2\vartheta = 35^\circ$ and $25^\circ$ shows the existence of Cu(II) in catalyst structure.

*EDS and MAP analysis*

In order to ensure the presence of expected elements in the catalyst structure, EDX analysis was used. EDX spectra taken at different points of the images are shown C, O, Cl, Fe and Cu elements in the catalyst (Fig. 4). In Fig. 4, the presence of the elements C, O, Cl, Fe and Cu with the corresponding weight percentages of 20.64, 61.88, 1.22, 6.06 and 10.20 % respectively is clearly evident the formation of $Fe_3O_4$@nano-coconut shell/Cu(II).

The distribution of the $Fe_3O_4$@nano-coconut shell/Cu(II) is also analyzed by elements mapping that shows C, O, Cl, Fe and Cu elements are distributed homogeneously in the synthesized catalyst (Fig. 5).

By measuring the Fe and Cu content in the catalyst using Inductively Coupled Plasma (ICP),

Table 1 Parameters obtained from porosity analysis

| | |
|---|---|
| BET Plot | |
| $V_m$ | 8.4111 [$cm^3$(STP) $g^{-1}$] |
| $a_{s,BET}$ | 36.609 [$m^2$ $g^{-1}$] |
| $C$ | 43.125 |
| Total pore volume($p/p_0$=0.990) | 0.1657 [$cm^3$ $g^{-1}$] |
| Mean pore diameter | 18.107 [nm] |
| Langmuir plot | |
| $V_m$ | 10.609 [$cm^3$(STP) $g^{-1}$] |
| $a_{s,Lang}$ | 46.174 [$m^2$ $g^{-1}$] |
| B | 0.2929 |
| t plot | |
| Plot data | Adsorption branch |
| $a_1$ | 27.312 [$m^2$ $g^{-1}$] |
| $V_1$ | 0 [$cm^3$ $g^{-1}$] |
| BJH Plot | |
| Plot data | Adsorption branch |
| $V_p$ | 0.1698 [$cm^3$ $g^{-1}$] |
| $r_{p,peak}$(*Area*) | 4.61 [nm] |
| $a_p$ | 49.768 [$m^2$ $g^{-1}$] |

Table 2. Synthesis of 4a under various conditions

| Entry | Catalyst amount (g) [d] | Solvent | Temp. (ºC) | Tim(min) | Yield% [b] |
|---|---|---|---|---|---|
| 1 | - | EtOH | r.t | 120 | Trace |
| 2 | - | EtOH | 80 | 100 | 25 |
| 3 | 0.05 | EtOH | r.t. | 100 | 53 |
| 4 | 0.05 | EtOH | 80 | 45 | 85 |
| 5 | 0.05 | $CH_3CN$ | 80 | 45 | 65 |
| 6 | 0.05 | $CH_3OH$ | 80 | 45 | 77 |
| 7 | 0.05 | Solvent free | 80 | 45 | 85 |
| 8 | 0.05 | Solvent free [a] | 80 | 15 | 96 |
| 9 | 0.05 | Solvent free [a] | r.t | 15 | 55 |
| 10 | 0.05 | Solvent free [a] | 60 | 15 | 74 |
| 11 | 0.05 | Solvent free [a] | 80 | 15 | 96 |
| 12 | 0.04 | Solvent free [a] | 80 | 15 | 96 |
| 13 | 0.03 | Solvent free [a] | 80 | 15 | 96 |
| 14 | 0.02 | Solvent free [a] | 80 | 15 | 88 |
| 15 | 0.00 | Solvent free [a] | 80 | 15 | - |

Reaction was performed with ethyl acetoacetate (1 mmol), benzaldehyde (1 mmol), dimedone (1 mmol), ammonium acetate (1.25 mmol).
[a] Electrical mortar-heater. [b] Isolated yield. $Fe_3O_4$@nano-coconut shell/Cu(II)[d]

we have found that the amount of Fe is 190 mg/g and Cu is 100 mg/g. Thus, according to ICP, the molar ratio of Cu:Fe is 1: 1.6.

*VSM magnetization study*

The magnetic properties of $Fe_3O_4$ and $Fe_3O_4$@ nano-coconut shell/Cu(II) was studied by using vibrating sample magnetometer (VSM) (Fig. 6). A super paramagnetic behavior was achieved from the measured samples of $Fe_3O_4$ and the catalyst. At room temperature, the saturation magnetization (*M*s) values of $Fe_3O_4$ and $Fe_3O_4$@nano-coconut shell/Cu(II) are ~50 emu $g^{-1}$ and ~32 emu $g^{-1}$, respectively. The resulting values show that bonding $Fe_3O_4$ @ nano-coconut shell/Cu(II) has considerable effect on the magnetic properties of $Fe_3O_4$.

*TGA analysis*

Thermal gravimetric analysis (TG-DTA) pattern of $Fe_3O_4$@nano- coconut shell/Cu(II) catalyst was shown in Fig. 7. A minor weight loss (10%) in the range of 50-280° can be related to remove the adsorbed water in catalyst. The other weight losses of the catalyst are occurred 30% in the range of 280-380 °C and 10% in the range of 630-650 °C are attributed to burning of carbohydrate section of catalyst. The char yield of catalyst at 800 °C is 39% that confirm the existence of metal in catalyst. Thus, the catalyst is stable up to 280 °C. and can be used under 280°C.

*SEM and TEM analysis*

To clarify the morphologies and sizes of the $Fe_3O_4$@nano-coconut shell/Cu(II), FESEM, TEM and histogram images of it were shown in Fig. 8. These results exhibit that the dimension of catalyst particles are 20-40 nm.

*Burunauer-Emmett-Taller (BET) analysis*

The Burunauer- Emmett- Taller specific surface area ($S_{BET}$) of the $Fe_3O_4$@nano-coconut shell/Cu(II) catalyst was measured by $N_2$ adsorption-desorption analysis at 77 K (Fig. 9 and Table 1). As shown, the $N_2$ adsorption- desorption isotherm for $Fe_3O_4$@nano-coconut shell/Cu(II) is of the II-type with $H_3$ hysteresis. As shown in Table 1, mean pore diameters and total pore volume were 18.107 nm, and 0.1657 cm3.$g^{-1}$, respectively.

*Application of $Fe_3O_4$@nano-coconut shell/Cu(II) in the synthesis of polyhydroquinolines*

In this investigation, we have synthesized polyhydroquinoline derivatives through MCRs using $Fe_3O_4$@nano-coconut shell/Cu(II). The reaction of benzaldehyde, dimedone, ethyl acetoacetate and ammonium acetate, to forming 4a, was done as model reaction for determination of the best reaction conditions. The resulted data about reaction solvent, temperature and the amount of the catalyst were tabulated in Table 2. Based on the obtained data, the model reaction under solvent free condition in electrical mortar-heater using 0.03 g of catalyst has higher yield than other conditions (Table 2, entry13).

Table 3 shows the comparison of $Fe_3O_4$@ nano-coconut shell/Cu(II) with the several other catalysts in the synthesis of (4a). The results showed that $Fe_3O_4$@nano-coconut shell/Cu(II) promotes the reaction with shorter reaction time and higher yield.

Finally, by applying the best condition, different polyhydroquinoline derivatives were prepared and the obtained results were tabulated in Table 4.

*Recyclability of the $Fe_3O_4$@ nano-coconut shell/ Cu(II)*

Reusability is one of the applied features of

Table 3. Catalytic performances of $Fe_3O_4$@nano- coconut shell/Cu(II) in comparison

| Entry | Catalyst | Solvent/conditions | Time(min) | Yield [a](%) | [Lit.] |
|---|---|---|---|---|---|
| 1 | AFGO nanosheets | EtOH, r.t. | 120-240 | 87-91 | [32] |
| 2 | MCM-41@serine@Cu(II) | EtOH, Reflux | 170 | 96 | [33] |
| 3 | KH2PO4 | EtOH:H2O/ 100 °C | 300 | 91 | [34] |
| 4 | TEDETA@BNPs | EtOH/ 80 °C | 60 | 95 | [35] |
| 5 | SBA-15@Glycine-M | EtOH/ | 110 | 92 | [36] |
| 6 | $Ga_2O_3$ nanomaterial | EtOH, Reflux | 60 | 90 | [37] |
| 7 | Ascorbic acid | Solvent free/ 80 °C | 1.5–5 h | 70-99 | [38] |
| 8 | Cu(II)-DCC-CMK-3 | solvent-free/80 °C | 25 | 98 | [39] |
| 9 | spinel FeAl2O4 | EtOH/ 80 °C | 30 | 96 | [40] |
| 10 | Aluminized polyborate | - | 15 | 94 | [41] |
| 11 | $Fe_3O_4$@nano-coconut shell/Cu(II) | under solvent-free/ 80 °C | 15 | 96 | Present work |

heterogeneous catalysts which is important from industrial and environmental view. To investigate this property, the retrieved catalyst from the reaction was reused for seven consecutive runs and results was presented in Fig. 10. These data show that the product yield was not reduced considerably after seven consecutive runs.

*Mechanism for the synthesis of polyhydroquinoline derivatives*

The proposed mechanism for the synthesis of polyhydroquinoline 4a in the presence of $Fe_3O_4$@

Table 4. Synthesis of polyhydroquinolines in the presence of $Fe_3O_4$@ nano-coconut shell/Cu(II)

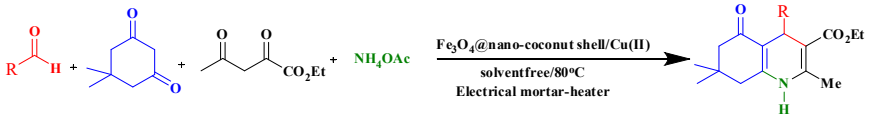


| Ent. | R | Prod. | Time (min) | Yield [b] (%) | M.P.(°C) Found | Lit. Mp (°C) [Refs.] |
|---|---|---|---|---|---|---|
| 1 |  | 4a | 20 | 96 | 223-224 | 223-225[31] |
| 2 |  | 4g | 15 | 92 | 196–197 | 196-198[31] |
| 3 | 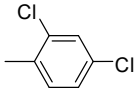 | 4h | 17 | 85 | 234–236 | 234-237[31] |
| 4 |  | 4j | 20 | 96 | 248–251 | 248-250[31] |
| 5 | 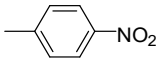 | 4n | 15 | 89 | 234–236 | 234-236[31] |
| 6 | 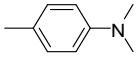 | 4b | 20 | 70 | 231-232 | 229-232[42] |
| 7 | 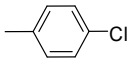 | 4f | 20 | | 234–235 | 234-235[43] |
| 8 | 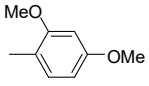 | 4i | 20 | 80 | 235-237 | 236-238[44] |
| 9 | 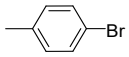 | 4c | 20 | 78 | 254–256 | 253-255[45] |
| 10 |  | 4e | 20 | 94 | 202–204 | 203-205[46] |
| 11 | 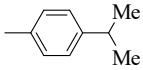 | 4q | 20 | 92 | 208-210 | 209-213[47] |
| 12 | 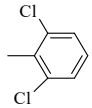 | 4d | 15 | 87 | 204-205 | 205-207 [31] |
| 13 |  | 4k | 20 | 84 | 218–220 | 219-221[43] |
| 14 | 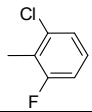 | 4l | 18 | 70 | 216-218 | 214-216 [45] |

Reaction was performed with ethyl acetoacetate (1 mmol), benzaldehyde (1 mmol), dimedone (1 mmol), ammonium acetate (1.25 mmol), $Fe_3O_4$@ nano-coconut shell/Cu(II) (30 mg). [b] Isolated yield.

nano-coconut shell/Cu(II) is shown in Fig. 11. As is shown, in the first and second steps, the carbonyl groups of the ethyl acetoacetate and aldehyde were activated by interactions with the Cu(II) on the catalyst. The active aldehyde reacts with dimedone via Knoevenagel condensation to formation of intermediate 9. On the other hand, intermediate 8 is formed during the condensation

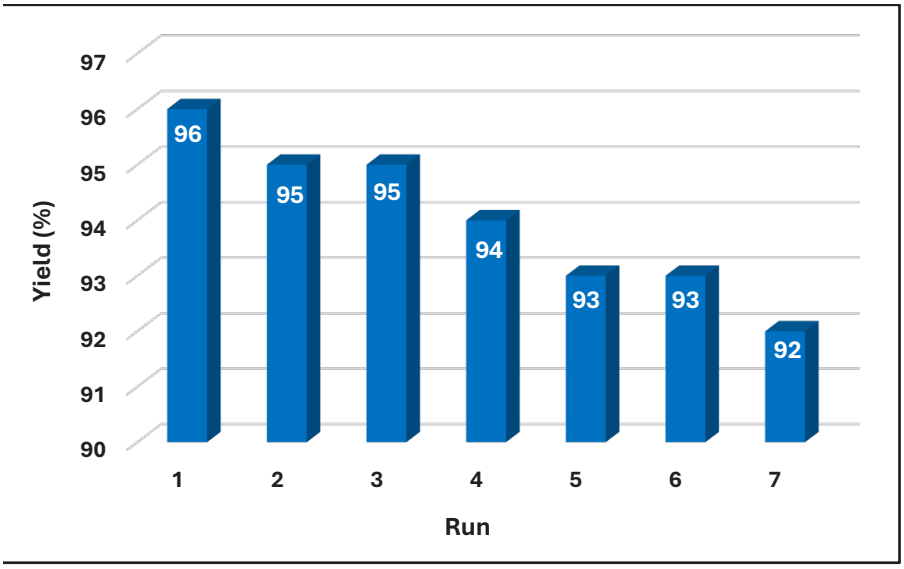


Fig. 10. Reusability of $Fe_3O_4$@ nano-coconut shell/Cu(II)

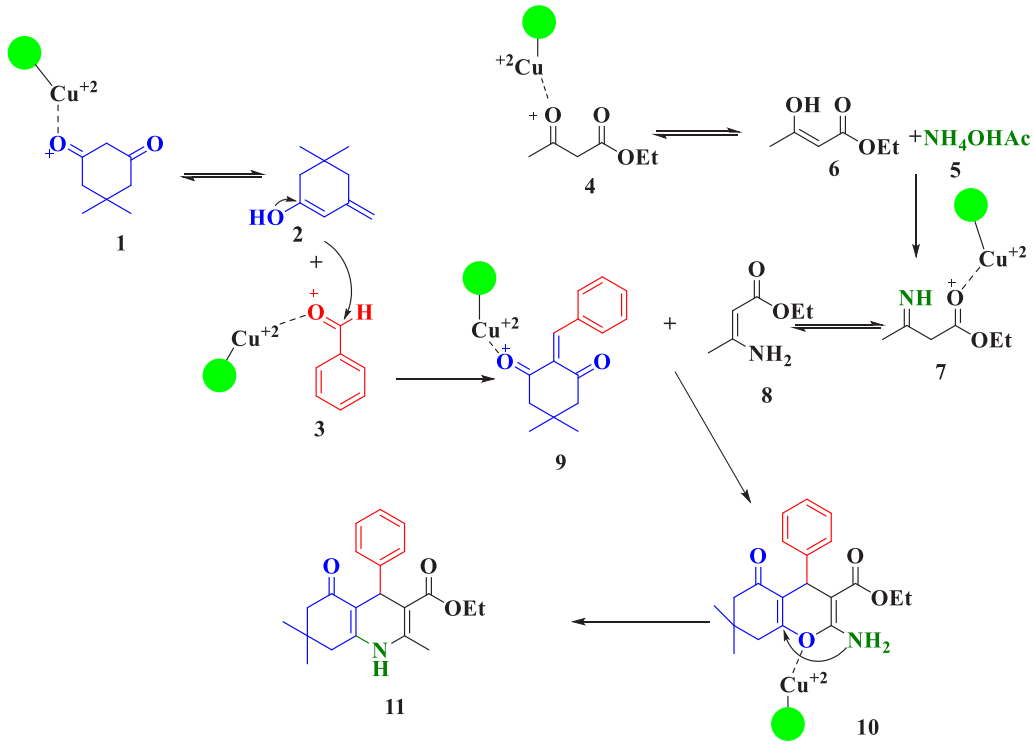


Fig. 11. Proposed mechanism for the synthesis of Polyhydroquinoline

reaction between the active ethyl acetoacetate and ammonium acetate. Then, Michael addition reaction between intermediates 9 and 8 forms the intermediate 10. Finally, polyhydroquinoline 11 is generated by an intramolecular nucleophilic reaction.

## CONCLUSION

In this work, $Fe_3O_4$@ nano-coconut shell/Cu(II) was introduced as a novel, green, efficient and magnetically removable solid acid catalyst for the synthesis of polyhydroquinoline derivatives. This protocol was done by using an electrical mortar-heater under solvent free condition. The reusability of catalyst, simplicity of procedure and high yields are some advantages of this protocol.

## ACKNOWLEDGEMENT

The Research Council of Yazd University is gratefully acknowledged for the financial support for this work.

## CONFLICT OF INTEREST

The authors declare that there is no conflict of interests regarding the publication of this manuscript.

## REFERENCES

1. Chen H, Wang Y. An Overview of Polysaccharides and the Influence Factors of Hypoglycemic Activity. Structure and Health Effects of Natural Products on Diabetes Mellitus: Springer Singapore; 2021. 163-177.
2. Shaabani A, Maleki A. Cellulose sulfuric acid as a bio-supported and recyclable solid acid catalyst for the one-pot three-component synthesis of α-amino nitriles. Applied Catalysis A: General. 2007;331:149-151.
3. Abdul Khalil HPS, Tye YY, Saurabh CK, Leh CP, Lai TK, Chong EWN, et al. Biodegradable polymer films from seaweed polysaccharides: A review on cellulose as a reinforcement material. Express Polymer Letters. 2017;11(4):244-265.
4. Cyras VP, Soledad CM, Analía V. Biocomposites based on renewable resource: Acetylated and non acetylated cellulose cardboard coated with polyhydroxybutyrate. Polymer. 2009;50(26):6274-6280.
5. Credou J, Berthelot T. Cellulose: from biocompatible to bioactive material. J Mater Chem B. 2014;2(30):4767-4788.
6. Cipriani G, Salvini A, Baglioni P, Bucciarelli E. Cellulose as a renewable resource for the synthesis of wood consolidants. J Appl Polym Sci. 2010;118(5):2939-2950.
7. Siró I, Plackett D. Microfibrillated cellulose and new nanocomposite materials: a review. Cellulose. 2010;17(3):459-494.
8. Lu Y, Lu X, Mayers BT, Herricks T, Xia Y. Synthesis and characterization of magnetic Co nanoparticles: A comparison study of three different capping surfactants. J Solid State Chem. 2008;181(7):1530-1538.
9. Rase HF, Hayes M. Commercial Heterogeneous Catalysis. Platinum Met Rev. 2001;45(2):83-83.
10. El Harrak A, Carrot G, Oberdisse J, Eychenne-Baron C, Boué F. Surface−Atom Transfer Radical Polymerization from Silica Nanoparticles with Controlled Colloidal Stability. Macromolecules. 2004;37(17):6376-6384.
11. Tartaj P, Serna CJ. Synthesis of Monodisperse Superparamagnetic Fe/Silica Nanospherical Composites. Journal of the American Chemical Society. 2003;125(51):15754-15755.
12. Azad S, Fatameh Mirjalili BB. $Fe_3O_4$ @nano-cellulose/TiCl: a bio-based and magnetically recoverable nano-catalyst for the synthesis of pyrimido[2,1-b]benzothiazole derivatives. RSC Advances. 2016;6(99):96928-96934.
13. Zhang Z, Duan H, Li S, Lin Y. Assembly of Magnetic Nanospheres into One-Dimensional Nanostructured Carbon Hybrid Materials. Langmuir. 2010;26(9):6676-6680.
14. Zolfigol MA, Moosavi-Zare AR, Moosavi P, Khakyzadeh V, Zare A. Nano-ferrous ferric oxide (nano-$Fe_3O_4$): Powerful, reusable, and stable catalyst for N-Boc protection of amines. Comptes Rendus Chimie. 2013;16(11):962-966.
15. Safajoo N, Mirjalili BBF, Bamoniri A. $Fe_3O_4$ @nano-cellulose/Cu(ii): a bio-based and magnetically recoverable nano-catalyst for the synthesis of 4 H-pyrimido[2,1-b] benzothiazole derivatives. RSC Advances. 2019;9(3):1278-1283.
16. Raju GB, Holmgren A, Forsling W. Complexation Mechanism of Dextrin with Metal Hydroxides. Journal of Colloid and Interface Science. 1998;200(1):1-6.
17. Liu Q, Laskowski JS. The interactions between dextrin and metal hydroxides in aqueous solutions. Journal of Colloid and Interface Science. 1989;130(1):101-111.
18. Angyal SJ. Complexes of Metal Cations with Carbohydrates in Solution. Advances in Carbohydrate Chemistry and Biochemistry: Elsevier; 1989. p. 1-43. http://dx.doi.org/10.1016/s0065-2318(08)60411-4
19. Gessa C, De Cherchi ML, Dessì A, Deiana S, Micera G. The reduction of Fe(III) to Fe(II) and V(V) to V(IV) by polygalacturonic acid: A reduction and complexation mechanism of biochemical significance. Inorg Chim Acta. 1983;80:L53-L55.
20. Anker L, Gopalakrishna R, Jones KD, Law RE, Couldwell WT. Hypericin in adjuvant brain tumor therapy. Drugs of the Future. 1995;20(5):511.
21. Chen Y-L, Fang K-C, Sheu J-Y, Hsu S-L, Tzeng C-C. Synthesis and Antibacterial Evaluation of Certain Quinolone Derivatives. J Med Chem. 2001;44(14):2374-2377.
22. Jadhvar SC, Kasraliker HM, Goswami SV, Chakrawar AV, Bhusare SR. One-pot synthesis and evaluation of anticancer activity of polyhydroquinoline derivatives catalyzed by [Msim]Cl. Res Chem Intermed. 2017;43(12):7211-7221.
23. Karimi Askarani H, Karimi Zarchi MA, Mirjalili BF, Bamoniri A. One-pot synthesis of polyhydroquinoline derivatives using nano-$Fe_3O_4$@dextrin/BF3 as a magnetic biodegradable catalyst. Journal of the Iranian Chemical Society. 2022;19(7):3189-3203.
24. Rathod S, Dhage V, Lande M. An eco-friendly synthesis of polyhydroquinoline derivatives using $MoO_3$ promoted CeO2-ZrO2 solid heterogeneous catalyst. Materials Today: Proceedings. 2021;47:1736-1740.
25. Dharma Rao GB, Nagakalyan S, Prasad GK. Solvent-free synthesis of polyhydroquinoline derivatives employing mesoporous vanadium ion doped titania nanoparticles as a robust heterogeneous catalyst via the Hantzsch reaction.

RSC Advances. 2017;7(6):3611-3616.
26. Rathod VN, Bansode ND, Thombre PB, Lande MK. Efficient one-pot synthesis of polyhydroquinoline derivatives through the Hantzsch condensation using IRMOF-3 as heterogeneous and reusable catalyst. J Chin Chem Soc. 2021;68(4):601-609.
27. Sheik Mansoor S, Aswin K, Logaiya K, Sudhan SPN. An efficient one-pot multi component synthesis of polyhydroquinoline derivatives through Hantzsch reaction catalysed by Gadolinium triflate. Arabian Journal of Chemistry. 2017;10:S546-S553.
28. Khabazzadeh H, Kermani ET, Afzali D, Amiri A, Jalaladini A. Efficient one-pot synthesis of polyhydroquinoline derivatives using Cs2.5H0.5PW12O40 as a heterogeneous and reusable catalyst in molten salt media. Arabian Journal of Chemistry. 2012;5(2):167-172.
29. Mondal S, Patra BC, Bhaumik A. One-Pot Synthesis of Polyhydroquinoline Derivatives through Organic-Solid-Acid-Catalyzed Hantzsch Condensation Reaction. ChemCatChem. 2017;9(8):1469-1475.
30. Yelwande AA, Navgire ME, Palve M, Patil HS, Farooqui M, Dinore JM. One-pot multicomponent synthesis approach for tetrahydropyridines using polyaniline-zirconium oxide composites. Synth Commun. 2022;52(7):1039-1049.
31. Sam M, Dekamin MG, Alirezvani Z. Dendrons containing boric acid and 1,3,5-tris(2-hydroxyethyl)isocyanurate covalently attached to silica-coated magnetite for the expeditious synthesis of Hantzsch esters. Sci Rep. 2021;11(1).
32. Choudhury P, Ghosh P, Basu B. Amine-functionalized graphene oxide nanosheets (AFGONs): an efficient bifunctional catalyst for selective formation of 1,4-dihydropyridines, acridinediones and polyhydroquinolines. Mol Divers. 2019;24(1):283-294.
33. Tamoradi T, Ghadermazi M, Ghorbani-Choghamarani A. Correction to: Synthesis of Polyhydroquinoline, 2,3-Dihydroquinazolin-4(1H)-one, Sulfide and Sulfoxide Derivatives Catalyzed by New Copper Complex Supported on MCM-41. Catal Lett. 2019;149(9):2645-2646.
34. Yü S-J, Wu S, Zhao X-M, Lü C-W. Green and efficient synthesis of acridine-1,8-diones and hexahydroquinolines via a KH2PO4 catalyzed Hantzsch-type reaction in aqueous ethanol. Res Chem Intermed. 2016;43(5):3121-3130.
35. Ghorbani-Choghamarani A, Heidarnezhad Z, Tahmasbi B, Azadi G. TEDETA@BNPs as a basic and metal free nanocatalyst for Knoevenagel condensation and Hantzsch reaction. Journal of the Iranian Chemical Society. 2018;15(10):2281-2293.
36. Tamoradi T, Ghorbani-Choghamarani A, Ghadermazi M, Veisi H. SBA-15@Glycine-M (M= Ni and Cu): Two green, novel and efficient catalysts for the one-pot synthesis of 5-substituted tetrazole and polyhydroquinoline derivatives. Solid State Sciences. 2019;91:96-107.
37. Parhad A, Aute D, Gadhave A, Uphade B. Gallium Oxide ($Ga_2O_3$): An Efficient Heterogeneous Nanocatalyst for One Pot, Multi-Component Synthesis of Polyhydroquinolines. Polycyclic Aromatic Compounds. 2021;42(8):5809-5823.
38. Sehout I, Boulcina R, Boumoud B, Boumoud T, Debache A. Solvent-free synthesis of polyhydroquinoline and 1,8-dioxodecahydroacridine derivatives through the Hantzsch reaction catalyzed by a natural organic acid: A green method. Synth Commun. 2017;47(12):1185-1191.
39. Ghafouri-Nejad R, Hajjami M. Synthesis and characterization of Cu–N, N′-Dicyclohexylcarbodiimide supported on CMK-3 as a novel, efficient and recoverable nanocatalyst for synthesis of tetrazole, polyhydroquinoline, and sulfoxide derivatives. Reaction Kinetics, Mechanisms and Catalysis. 2019;129(1):371-389.
40. Ghorbani-Choghamarani A, Mohammadi M, Shiri L, Taherinia Z. Synthesis and characterization of spinel FeAl2O4 (hercynite) magnetic nanoparticles and their application in multicomponent reactions. Res Chem Intermed. 2019;45(11):5705-5723.
41. Aute D, Kshirsagar A, Uphade B, Gadhave A. Aluminized polyborate-catalysed green and efficient synthesis of polyhydroquinolines under solvent-free conditions. Res Chem Intermed. 2020;46(7):3491-3508.
42. Kardooni R, Kiasat AR, Motamedi H. Designing of a novel dual-function silica-iron oxide hybrid based nanocomposite, $Fe_3O_4$ @$SiO_2$ PEG/$NH_2$, and its application as an eco-catalyst for the solvent-free synthesis of polyhydroacridines and polyhydroquinolines. Journal of the Taiwan Institute of Chemical Engineers. 2017;81:373-382.
43. Waghmare AS, Kadam KR, Murade VD, Pandit SS. Microwave Assisted One-Pot Three-Component Synthesis Of 3,4-Dihydropyrimidin-2(1h)-Ones Using Sfhs as an Efficient and Reusable Catalyst. Rasayan Journal of Chemistry. 2022;15(01):668-675.
44. Singh H, Garg N, Arora P, Rajput JK, Jigyasa. Sucrose chelated auto combustion synthesis of $BiFeO_3$ nanoparticles: Magnetically recoverable catalyst for the one-pot synthesis of polyhydroquinoline. Appl Organomet Chem. 2018;32(6).
45. Vahdat SM, Chekin F, Hatami M, Khavarpour M, Baghery S, Roshan-Kouhi Z. Synthesis of polyhydroquinoline derivatives via a four-component Hantzsch condensation catalyzed by tin dioxide nanoparticles. Chinese Journal of Catalysis. 2013;34(4):758-763.
46. Ghorbani-Choghamarani A, Heidarnezhad Z, Tahmasbi B. New Complex of Copper on Boehmite Nanoparticles as Highly Efficient and Reusable Nanocatalyst for Synthesis of Sulfides and Ethers. ChemistrySelect. 2019;4(30):8860-8869.
47. Choudhury P, Basu B. Graphene oxide nanosheets as sustainable carbocatalysts: Synthesis of medicinally important heterocycles. Green Approaches in Medicinal Chemistry for Sustainable Drug Design: Elsevier; 2020. p. 47-74.